The Latest Progress on Electron Transfer in Macromolecule-Metal Complexes and Future Scope of MMC

Eishun Tsuchida*

Department of Polymer Chemistry, Advanced Research Institute for Science & Engineering, Waseda University, Tokyo 169-8555, Japan.

CREST investigator, JST.

SUMMARY: We have been developing a method to regulate the electronic processes of the O_2-coordinated metal complexes using macromolecules, including synthetic polymers, molecular assemblies, and multi-nuclear complexes. Acceleration of the electron transfer leads a variety of molecular conversions. Mixed valent vanadyl complexes, for example, act as a multi-electron transfer mediator for the oxidative polymerization of the diphenyl disulfide, and a pure and high molecular weight poly(thiophenylene) can be obtained. At the same time, the dinuclear vanadium complex acts as an efficient catalyst for the four-electron reduction of dioxygen to water. We have recently expanded this reaction to other μ-oxo dimeric complexes. On the other hand, prevention of the electron transfer process increases the stability of the O_2-adduct compounds. The tetraphenylporphyrinato-iron(II) derivative incorporated into human serum albumin can reversibly bind and release dioxygen under physiological conditions (in aqueous media, pH 7.3, 37°C) like hemoglobin and myoglobin. The micro-environment around the porphyrinatoiron in the albumin structure retards the irreversible oxidation of the central iron(II). The O_2-binding ability of this synthetic hemoprotein satisfies the clinical requirements for O_2-infusion as a red blood cell substitute.

Introduction

The most significant role of the macromolecules in *Macromolecule-Metal Complexes (MMC)* is construction of a micro-environment around the complex moiety, which can perform the molecular recognition and condensation.[1-3] The second part is to control the electronic process of the central metals. In nature, there are numerous examples of macromolecule-metal complexes; *e.g.*, metallo-enzymes and metallo-proteins. The polymer matrices, namely polypeptides, surrounding the active sites directly or indirectly influence the metal complexes, and acceleration or prevention of the electronic process on the metal center affords efficient reactions which cannot be seen in a homogeneous solution. Of course, these processes observed in biological systems have been established through molecular evolution over a long time period. Cytochrome *c* oxidaze

 CCC 1022-1360/00/$ 17.50+.50/0

is typical MMC performing the acceleration of electron transfer. Since its crystal structure was solved in 1995,[4,5] the reaction mechanism of this hemoprotein, i.e., four electron reduction of dioxygen molecule, is of current interest. However, there are still many discussions concerning the role of the copper ion on the porphyrin plane. On the other hand, in hemoglobin and myoglobin, the electron transfer of the coordinated dioxygen is suppressed. The heme moiety is incorporated into the hydrophobic domain of the globin chain, and surrounded by the molecular environment, so called the *hemepocket*, which prevents the unfavorable irreversible oxidation of the central iron(II). If one can realize these extremely efficient reactions observed in metallo-proteins using synthetic polymers, the design of the chemical reactions will be essentially changed. This is one of the most significant challenges in recent macromolecular science. In this paper, we describe the latest progress in the regulation of the electron transfer process in O_2-coordinated MMC.

Catalysts of O_2-Reduction by μ-Oxo Dinuclear Complexes

a. Role of Multi-Electron Redox Catalysts

A number of metal complexes have been used as catalysts for the electroreduction of dioxygen.[6] The catalytic reactions in acidic media facilitate the O_2 reduction via the four-electron reduction to H_2O and the two-electron transfer to produce partially reduced H_2O_2. Of more importance is the catalyst for the selective four-electron reduction of O_2 to H_2O without the formation of the partially reduced active oxygen species, since the four-electron reduction catalyst provides not only a clean energy transformation system such as those in biological respiratory systems, but also redox systems for synthetic processes such as the oxidative polymerization of organic compounds using O_2 as an abundant oxidant[7-11] We have established a novel catalytic process of vanadium complexes for the O_2-oxidative polymerization of disulfide and sulfides, which provides a linear high molecular-weight poly(thio-1,4-phenylene) at room temperature. Attention has been focused upon the development of multi-electron redox catalysts for the four-electron reduction of O_2.[12,13] Herein, emphasis is placed on our finding that μ-oxo dinuclear complexes can be versatile and convenient electrocatalysts for the four-electron reduction of O_2.

b. Multi-Electron Process of μ-Oxo Dinuclear Complexes

One of the most important conclusions derived from the series of pioneering work by Savy[14] and Barendrecht[15] is that dimeric (or polymeric) phthalocyanine species appear to be responsible for the marked catalytic activity, but the active dimeric (or polymeric)

species have not been structurally characterized. On the other hand, our preliminary work on iro-porphyrin complexes have revealed that a significant increase in the selectivity of four-electron reduction of O_2 is noticed for carbon electrodes adsorbed with O_2-bridged diiron(III)-porphyrins as compared to those with mononuclear iron-porphyrins. The implication is that the electroreduction of the adsorbed oxo-bridged dimer gives a cofacial geometry for the iron(II)-porphyrin on the electrode, thus facilitating the coordination and splitting of O_2. We report that the same is true for phthalocyanine complexes. Thus the electroreduction of an O_2-bridged phthalocyanine complex PcFe(III)-O_2-Fe(III)Pc adsorbed at a cathode surface under acidic conditions produces the two solid state, cofacially oriented molecules of iron(II)-phthalocyanine which are fixed at the solid support, allowing an accommodation of an O_2 molecule between the two iron(II) atoms and subsequent facile splitting of the O=O bond to produce two molecules of H_2O. As a result, the proportion of H_2O as a reduced product significantly increased for the adsorbed dimer.

c. Catalytic Four-Electron Reduction of O_2

The voltammogram for the reduction of O_2 at the uncoated electrode is shown in Fig. 1(a). The presence of a quasi-reversible voltammetric response near 0.3 V (vs. SCE) is a feature common to all carbon electrodes. The direct reduction of O_2 at an uncoated electrode was observed at potentials more negative than -0.5 V (vs. SCE). In Fig. 1(b), the dotted curve shows the typical steady-state current potential responses obtained at a glassy carbon electrode adsorbed with the μ-peroxo diiron(III)-phthalocyanine in argon-saturated aqueous acidic solutions. A redox couple was observed near 0.38 V (vs. SCE) in the voltammogram. Without acid, no redox wave was observed in the potential range from +0.8 down to negative potentials of at least 0 V (vs. SCE).

When the electrode was transferred to an O_2 saturated solution, a large catalytic current appeared near 0.32 V (vs. SCE) (Fig. 1(b), solid curve). Potential step chronocoulometry measurements revealed that the reduction under O_2-free conditions required ≈2 F per mole of iron adsorbed at the surface of the electrode (eq. (1)), which was almost quantitatively recovered upon exposure of the electrode to O_2.

$$[\text{PcFe(III)-O-O-Fe(III)Pc}]_{ad} + 4H^+ + 4e^- \rightarrow [\text{PcFe(II)}\quad\text{Fe(II)Pc}]_{ad} + 2H_2O \qquad (1)$$

$$\text{at } E^f = 0.39 - 0.059\text{pH (V vs SCE, pH>1.1)}$$

d. In-situ Structural Analysis and Catalytic Mechanism

Fig. 2 shows the Raman spectra of the electrode surface modified by the μ-peroxo diiron(III)-phthalocyanine. Comparison with a previous study[16] allows one to ascribe the broad peak at 788 cm^{-1} (Fig. 2(a)) to the Fe-O-O-Fe bond; the Raman shift is in accordance with the frequency observed for the axial base-coordinated O_2 adducts, which indicates that the pyridine molecules originally introduced as the axial ligand would be preserved during the course of the measurement. The peak disappeared upon reduction under acidic media in the absence of O_2 (Fig. 2(b)) as a result of the reductive cleavage of the O-O bond (eqn. (1)). When the electrode is subsequently soaked into oxygen-saturated water in the absence of acid, the more pronounced peaks due to the μ-peroxo bond appeared at 788 and 810 cm^{-1} as shown in Fig. 2(c). The Raman shift of the latter peak is in accordance with the frequency observed for the axial base-free O_2 adducts. Substitution of $^{16}O_2$ with $^{18}O_2$ induced a low-frequency shift (40 cm^{-1}) as shown in Fig. 2(d). The isotope shift is in good agreement with that expected for a O-O harmonic oscillator (45 cm^{-1}) of the peroxo bridged structure. The oxygenation-deoxygenation cycle can be repeated without any significant

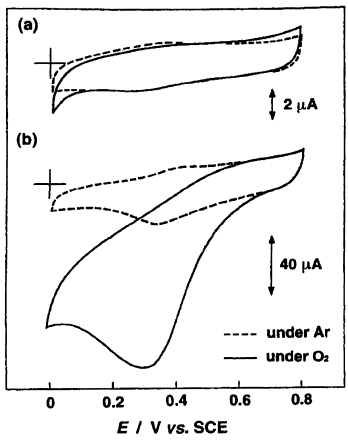

Fig. 1 Cyclic voltammograms at (a) a bare glassy carbon electrode (A = 0.28 cm^2), (b) the same electrode coated with 8.4×10^{-2} mg/cm^2 (1.8×10^{-8} mol/cm^2) of pyPcFe(III)-O_2-Fe(III)Pc py. Supporting electrolyte was 0.1 mol/L NH_4PF_6 aqueous solution containing 0.5 mol/L $HClO_4$. Potential sweep rate was 50 mV/s.

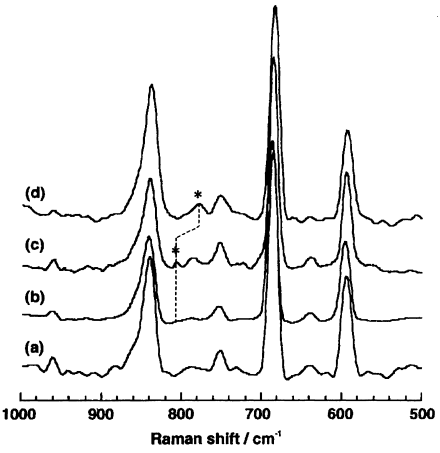

Fig. 2 Raman spectra of (a) the glassy carbon electrode modified with pyPcFe(III)-O_2-Fe(III)Pcpy (1.8×10^{-8} mol/cm^2). (b) Repeat of (a) after the electrode was immersed in an aqueous electrolyte solution containing 0.1 mol/L NH_4PF_6 and 0.5 mol/L $HClO_4$ under argon and the adsorbate was reduced at 0 V. (c) Repeat of (b) after the electrode was immersed in H_2O saturated with $^{16}O_2$. (d) Repeat of (b) after the electrode was immersed in H_2O saturated with $^{18}O_2$.

decrease in the peak intensity, which indicates that the original orientation of the Pc rings at the electrode surface is preserved throughout the cycle due to the restricted dynamics on the solid support. In controlled experiments using the mononuclear PcFe(II) as an adsorbate, intensity of the peak due to the μ-peroxo bond produced upon oxygenation was much smaller as expected for the adsorption of the molecule without the cofacial orientation.

In conclusion, the electroreduction of O_2 at a carbon electrode adsorbed with a μ-peroxo diiron(III) phthalocyanine proceeds by the coordination of O_2 between the two proximal iron(II) centers which are produced by the reduction of the μ-peroxo diiron(III) center under acidic conditions. The modified electrode allowed 84% of the O_2 to be reduced to H_2O by a four-electron reduction (Scheme 1).

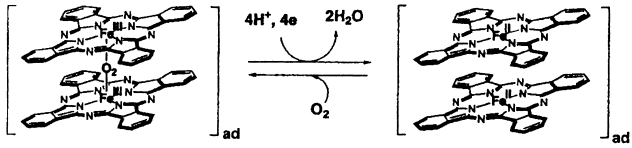

Scheme 1

Reversible O_2-Binding of Human Serum Albumin-Heme Hybrid

On the other hand, the prevention of electron transfer on the O_2-coordinated complex realizes the formation of stable O_2-adduct compounds. The latest successful example is the human serum albumin-heme hybrid as a synthetic O_2-carrying hemoprotein.[17-20] Its O_2-binding abilities satisfy the clinical requirements for O_2 infusion as a red blood cell substitute. Human serum albumin (HSA, Fig. 3(a)) is the major transport protein which is able to bind a great variety of metabolites and organic compounds in our bloodstream.[21] We have recently found that a tetraphenylporphinatoiron(II) derivative with a covalently linked axial base, 2-[8-{N-(2-methylimidazolyl)}octanoyloxymethyl]-5,10,15,20-tetrakis (α,α,α,α-*o*-pivalamido)phenylporphinatoiron(II) (FeP) (Fig. 3(b)) is efficiently incorporated into the natural HSA or recombinant HSA. The obtained HSA-FeP hybrid can reversibly bind and release dioxygen under physiological conditions (in aqueous media, pH 7.3, 37 °C) in a fashion similar to hemoglobin and myoglobin.

a. Binding Aspects of FeP to HSA.

From the quantitative analyses of the free FeP in the prepared HSA-FeP solution, the maximum binding ratios of FeP to HSA were calculated to be eight.[18] The magnitude of the binding constants for the FeP association with HSA ($K_1 \sim K_8$) ranged from 1.2×10^6 to 1.3×10^4 M^{-1} in which no cooperative relation was observed.[19] These values are relatively low with respect to those of palmitic acid ($K_1 \sim K_8 = 6.2 \times 10^7 \sim 3.8 \times 10^5$ M^{-1}) and hemin ($K_1 = 5.0 \times 10^7$ M^{-1}), which have coulombic interactions with the albumin host molecules. Three of the eight association sites of FeP were estimated to be the IB-IIA, IIA, and IIIB subdomains from the competitive binding inhibition behavior by other well-known ligands.[22]

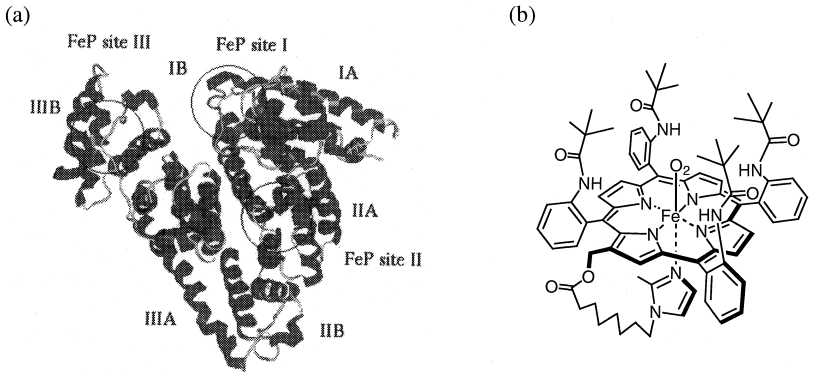

Fig. 3 (a) Three dimensional structure of HSA. The circles are the predicted binding sites of FeP. (b) Synthetic heme; FeP.

b. Solution and Physicochemical Properties.

The red-colored solution could be stored for three months at 4°C and no aggregation was observed for all prepared samples. Furthermore, the solution could be kept as a freeze-dried powder for more than six months. The long stability and no blood type, of course, are great advantages of this solution as a O_2 infusion for potential clinical use. The isoelectric points (pI) of the HSA-FeP (FeP/HSA = 1~8 (mol/mol)) were all found to be 4.8 based on the IEF measurements, these values were exactly the same as that of HSA itself.[18-19]

Circular dichroism (CD) spectroscopy provides information on the secondary and tertiary structures of HSA and conformation changes that ensue when FeP is bound. This spectral pattern showed typical double-minimum negative peaks in the ultraviolet region

independent of the binding numbers of the FeP molecules from one to eight. There are no differences between the HSA-FeP series and HSA itself.[19,20] The calculated α-helix content was approximately 60%, suggesting that the FeP association did not cause any second- and third-ordered structural changes in HSA.

c. O_2-Binding Properties of HSA-FeP.

The UV-vis. absorption spectrum of the aqueous HSA including the carbonyl FeP complex (FeP(CO)) showed a typical CO-coordinated low-spin tetraphenylporphinato-iron(II) derivative (λ_{max}: 424, 540 nm). Light irradiation with a 500-W incandescent lamp of this solution under O_2 allowed CO dissociation thus producing the dioxygenated species (λ_{max}: 424, 548 nm). Upon exposure of HSA-FeP(O_2) to argon, the UV-vis. absorption spectrum immediately changed to that of a five-N-coordinated species (λ_{max}: 439, 542, 563, 605 nm). This dioxygenation was reversible and kinetically stable under physiological conditions (pH 7.3, 37 ^{o}C) depending on the O_2-partial pressure.[18,20]

In the Resonance Raman spectra of the HSA-FeP solution under argon, there was a medium band at 201 cm^{-1}, which was assigned to the Fe(II)-N(imidazole) stretching mode, ν(Fe-N_ε), based on a similar assignment for other porphyrinatoiron(II) systems. After exposure to O_2, a new ν(Fe-O_2) vibration of dioxygenated FeP appeared at 564 cm^{-1}. This frequency suggests a typical end-on type O_2 coordination to the porphyrinatoiron(II). The deformation modes of the porphyrin ring (ν_8 and ν_4) were also immediately upshifted from 376 and 1356 cm^{-1} to 393 and 1371 cm^{-1}, respectively. These observations indicate the conversion of the five-coordinated high-spin state to the six-coordinated low-spin state of FeP. All the observed shifts changed reversibly depending on the O_2 concentration.[19] Therefore, it is concluded that the HSA-FeP definitely binds and releases an O_2 molecule in aqueous solution.

The O_2-binding affinities [$P_{1/2}$: gaseous pressure at half O_2-binding for the porphyrinatoiron(II)] of the HSA-FeP were determined on the basis of the UV-vis. spectral changes by O_2 titration.[19-20] The isosbestic points were maintained in all cases. It is remarkable that the values of $P_{1/2}$ were almost independent of the numbers of the associated FePs to HSA and rHSA (Table 1). The O_2-binding profile did not show any cooperativity like that seen in hemoglobin; the Hill coefficient was 1.0. Although the $P_{1/2}(O_2)$ values are relatively lower than that of hemoglobin, the O_2-transporting efficiency (OTE) of HSA-FeP between the lungs [$P(O_2)$: 110 Torr] and muscle tissue [$P(O_2)$: 40 Torr] becomes 22%,

which is nearly the same value (23%) as that of the red blood cells. The physiological responses and *in vivo* O_2 delivery of these serum albumin-heme hybrids in hemorrhagic shocked rats have also been evaluated.[23)]

Table 1. O_2-Binding affinities [$P_{1/2}(O_2)$] and O_2 solublity of HSA-FeP series.

	$P_{1/2}(O_2)$/ Torr		O_2-Solubility
	25°C	37°C	/ ml/dl
HSA-FeP(4)	14	32	10.5
HSA-FeP(8)	13	33	18.0
rHSA-FeP(4)	13	36	10.5
rHSA-FeP(8)	14	34	10.5
$(rHSA\text{-}FeP)_2$(16)	12	30	32.8
Red blood cell	9	27	25.9

d. Human Serum Albumin Dimers incorporating Sixteen FePs.

Although HSA-FeP is a new synthetic O_2-carrying molecule, the HSA-FeP solution with a physiological HSA concentration (5 g dL^{-1}) can involve only 6 mM heme, which corresponds to 60% of the whole blood ([heme]: 9.2 mM). Of course, a highly condensed solution can dissolve more FeP, but the colloid osmotic pressure increases in proportion to the HSA content. More recently, we have synthesized a new crosslinked rHSA hybrid incorporating *sixteen* FeP molecules as O_2-binding sites [$(rHSA\text{-}FeP)_2$].[24)] The O_2-binding affinity ($P_{1/2}$: 30 Torr, 37 °C) was almost the same as that of HSA-FeP and also satisfies the requirements for a synthetic O_2 carrier as a red blood cell substitute (Table 1). The $(rHSA\text{-}FeP)_2$ solution (10 g dL^{-1}) can dissolve the same amount of dioxygen relative to the whole blood under the physiological conditions expected in vivo.

Conclusions

The latest results on the regulation of electronic process on our MMC systems have been described. Acceleration of the electron transfer in well-difined dinuclear metal complexs leads an efficient molecular conversions. On the other hand, prevention of the electron transfer gives a stable O_2-infusion as a red blood cell substitute. As I indicated at the beginning, if one can realize the reactions in nature, for example metallo-proteins, using synthetic polymers, the design of the chemical reactions will be essentially changed. This is one of the most significant challenges in the modern macromolecular science.

Acknowledgment

This work was partially supported by the Core Research for Evolutional Science and Technology, JST, and Health Science Research Grants (Artificial Blood Project) of the Ministry of Health and Welfare, Japan.

References

1. Macromolecular Complexes "Dynamics Interactions and Electronic Processes" ed. E. Tsuchida, VCH Publishers, Inc., New York 1991.
2. Macromolecule-Metal Complexes, F. Ciardelli, E. Tsuchida, D. Wöhrle, (Eds.) SpringerVerlag, Berlin 1996.
3. E. Tsuchida, *Macromol. Symp.*, **131**, 155 (1998)
4. S. Iwata, C. Ostermeier, B. Ludwig, H. Michel, *Nature*, **376**, 660 (1995)
5. K. Tsukihara, H. Aoyama, E. Yamashita, T. Tomizaki, H. Yamaguchi, K. Shinzawa-Itoh, R. Nakashima, R. Yaono, S. Yoshikawa, *Science*, **269**, 1069 (1995)
6. K. Kinoshita, *Electrochemical Oxygen Technology*, John Wiley & Sons Inc., New York 1992.
7. K. Yamamoto, E. Tsuchida, H. Nishide, M. Jikei, K. Oyaizu, *Macromolecules*, **26**, 3432 (1993).
8. E. Tsuchida, K. Yamamoto, K. Oyaizu, *J. Electroanal. Chem.*, **438**, 167 (1997).
9. E. Tsuchida, K. Yamamoto, K. Oyaizu, F. Suzuki, H. Nishide, A. S. Hay, Z. Y. Wang, *Macromolecules*, **28**, 409 (1995).
10. E. Tsuchida, K. Yamamoto, M. Jikei, H. Nishide, *Macromolecules*, **22**, 4138 (1989).
11. K. Oyaizu, E. Tsuchida, *J. Am. Chem. Soc.*, **120**, 237 (1998).
12. K. Yamamoto, K. Oyaizu, E. Tsuchida, *J. Am. Chem. Soc.*, **118**, 12665 (1996).
13. K. Oyaizu, K. Yamamoto, K. Yoneda, E. Tsuchida, *Inorg. Chem.*, **35**, 6634 (1996).
14. A. Biloul, O. Contamin, G. Scarbeck, M. Savy, *J. Electroanal. Chem.*, **365**, 239 (1994).
15. A. Elzing, A. van der Putten, W. Visscher, E. Barenrecht, *J. Electroanal. Chem.*, **233**, 113 (1997).
16. B. Simic-Glavaski, S. Zecevic, E. Yeager, *J. Electroanal. Chem.*, **150**, 469 (1983).
17. Komatsu, K. Ando, N. Kawai, H. Nishide, E. Tsuchida, *Chem. Lett.*, **1995**, 813 (1995).
18. E. Tsuchida, K. Ando, H. Maejima, N. Kawai, T. Komatsu, S. Tekeoka, H. Nishide, *Bioconjugate Chem.* **8**, 534 (1997).
19. T. Komatsu, K. Hamamatsu, J. Wu, E. Tsuchida, *Bioconjugate Chem.* **10**, 83 (1999).
20. T. Komatsu, Y. Matsukawa, K. Hamamatsu, J. Wu, E. Tsuchida, *Bioconjugate Chem.* **10**, 797 (1999).
21. Peters Jr., T. *All about Albumin, Biochemistry, Genetics, and Medical Applications*, Academic Press, San Diego 1997, and references therein.
22. Kragh-Hansen, U. *Pharmacological Reviews* **1981**, *33,* 17.
23. E. Tsuchida, T. Komatsu, K. Hamamatsu, Y. Matsukawa, A. Tajima. A. Yoshizu, K. Kobayashi, *Bioconjugate Chem.* **10**, (1999) in press.
24. T. Komatsu, K. Hamamatsu, E. Tsuchida, *Macromolecules* **32** (1999) in press.